Monte Carlo Solution of Nonlinear Vibrations

M. SHINOZUKA* AND Y.-K. WEN†
Columbia University, New York

A Monte Carlo technique is presented which can effectively be used for nonlinear response analysis of a structure subjected to a random pressure field undergoing large deflections. The pressure field is idealized as a multidimensional Gaussian process with mean zero and homogeneous both in time and space. The response analysis is performed in the time domain by numerically simulating generalized forces rather than in the frequency domain. The solution satisfies the boundary conditions and the differential equation in a Galerkin sense. Two numerical examples involving large deflections of a string and a plate are worked out. The result indicates that the present method indeed provides a powerful tool in solving nonlinear structural response problems under random excitations.

Nomenclature

$\tilde{u}$ = u/U
L = string length
T_o = initial tension
$f(\bar{x},\bar{t})$ = force/unit length
η = coefficient of linear viscous damping
A = cross-sectional area of string
U = reference displacement
$\bar{w}$ = w/h
$\bar{y}$ = y/b
h = plate thickness
D = $Eh^3/12(1-\nu^2)$
ν = poisson ratio
$\bar{\nabla}^4$ = $[(b/a)(\partial^2/\partial\bar{x}^2)+(a/b)(\partial^2/\partial\bar{y}^2)]^2$
$\bar{p}$ = $(a^2b^2/\pi^2hD)p(\bar{x},\bar{y},\bar{t})$
$p(\bar{x},\bar{y},\bar{t})$ = pressure, three-dimensional homogeneous Gaussian process
λ = $\eta ab/\pi(\rho hD)^{1/2}$
ω' = $\omega\delta^*/U_o$
δ^* = displacement thickness
q_o = dynamic pressure $(1/2)\rho U_o^2$
$|R_{pp}(\xi,\eta,\omega)|$ = correlation coefficient = $\exp[-0.1\omega\xi/U_c(\omega)]\exp[-0.715\omega\eta/U_c(\omega)]$
U_o = freestream velocity
$U_c(\omega)$ = convection speed, a weak function of ω and regarded as constant here = $0.65U_o$
$\bar{\omega}$ = ωT (T; period of first mode of the plate)
$\bar{\delta}^*$ = δ^*/a
$\bar{U}_o$ = U_oT/a
$\bar{k}_1,\bar{k}_2$ = nondimensional wave number in x and y directions

I. Introduction

THE purpose of the present study is to present a Monte Carlo technique which can efficiently be used for the response analysis of a nonlinear structure subjected to a random pressure field. The nonlinearity considered is due to large deflections and not due to nonlinear stress-strain relationships. The pressure field is idealized as a multidimensional Gaussian process homogeneous both in time and space. The mean value of the process is assumed to be zero since as usual the structural response to the fluctuating part of the pressure is at issue here.

The principal idea is to perform the analysis in the time domain by simulating generalized forces rather than in the frequency domain as usually done in the linear response analysis. The solution satisfies the boundary conditions and the differential equations in a Galerkin sense. The time domain analysis in conjunction with the Monte Carlo technique for the solution of structural response involving geometrical nonlinearity appears to have been used first by Dowell[1] dealing with a simply supported rectangular plate subjected to a turbulent pressure field on one side and to a cavity pressure on the other with the interaction of the plate and external and/or internal (cavity) airflow being taken into consideration. In this study, however, Dowell simulated a pressure field which is white in one direction and uniform in the other. Such a process is unrealistic, as Dowell himself pointed out.

The present paper represents a major breakthrough in this time-domain approach since it incorporates into the dynamic analysis an efficient method of simulating a multidimensional Gaussian pressure field with a specified generalized spectral density. The method does not require filtering random processes and therefore is free from finding appropriate filters and performing convolution integrals.

II. Simulation of Random Processes

The essential feature of simulation is as follows: Consider a multidimensional homogeneous Gaussian process

$$f_o(x_1,x_2,\ldots,x_n)$$

with the auto-correlation function;

$$R_o(\xi_1,\xi_2,\ldots,\xi_n)=E[f_o(x_1,x_2,\ldots,x_n)\cdot f_o(x_1+\xi_1,x_2+\xi_2,\ldots,x_n+\xi_n)] \quad (1)$$

Because of the homogeneity of the process, the generalized spectral density $\Phi_o(\omega_1,\omega_2,\ldots,\omega_n)$, the n-fold Fourier transform of $R_o(\xi_1,\xi_2,\ldots,\xi_n)$, is real and non-negative. Then, the process $f_o(x_1,x_2,\ldots,x_n)$ can be simulated as

$$f(x_1,x_2,\ldots,x_n)=\sigma\left(\frac{2}{N}\right)^{1/2}\sum_{k=1}^{N}\cos(\omega_{1k}x_1+\ldots\omega_{nk}x_n+\Phi_k) \quad (2)$$

with Φ_k being uniformly distributed between 0 and 2π and independent of Φ_j for $k\neq j$ and with $\omega_{ik},\ldots,\omega_{nk}$ being random variables independent of $\omega_{ij},\ldots,\omega_{nj}$ for $k\neq j$ and of Φ_j and distributed according to the joint density function

$$g_n(\omega_1,\omega_2,\ldots,\omega_n)=\Phi_o(\omega_1,\omega_2,\ldots,\omega_n)/\sigma^2 \quad (3)$$

where

$$\sigma^2=\int_{-\infty}^{\infty}\ldots\int_{-\infty}^{\infty}\Phi_o(\omega_1,\omega_2,\ldots,\omega_n)\,d\omega_1\,d\omega_2\ldots d\omega_n \quad (4)$$

In a recent paper[2] by one of the present authors, this method of simulation of multivariate as well as multidimensional pro-

Presented as Paper 71-213 at the AIAA 9th Aerospace Sciences Meeting, New York, January 25–27, 1971; submitted December 10, 1970; revision received September 1, 1971. This study was supported by the National Science Foundation under GK 3858.

Index category: Structural Dynamic Analysis.

* Professor of Civil Engineering, Department of Civil Engineering and Engineering Mechanics. Member AIAA.

† Research Assistant, Department of Civil Engineering and Engineering Mechanics; presently Visiting Assistant Professor, Department of Civil Engineering, University of Illinois, Urbana, Ill.

cesses is described in detail. Also, Ref. 2 shows that the process $f(x_1, x_2, \ldots, x_n)$ is asymptotically ergodic as $N \to \infty$. Therefore, by using an appropriately large N, one can expect the simulated process to be ergodic and Gaussian at least in approximation, the latter being because of the central limit theorem.

The validity of the present approach is demonstrated in terms of the response analysis of a nonlinear string and a nonlinear plate.

III. Response of a Nonlinear String

The differential equation and the boundary conditions for transverse displacement u of a string under initial tension T_o are, in dimensionless form, given by

$$\frac{\partial^2 u}{\partial t^{-2}} + 2\beta\frac{\partial \bar{u}}{\partial \bar{t}} = 4\left[1 + \frac{AE}{2T_o}\left(\frac{U}{L}\right)^2 \int_0^1 \left(\frac{\partial \bar{u}}{\partial \bar{t}}\right)^2 d\bar{x}\right] \frac{\partial^2 \bar{u}}{\partial \bar{x}^2} + 4\left(\frac{L}{U}\right)\bar{f}(\bar{x}, \bar{t}) \tag{5}$$

$$\bar{u}(0, t) = \bar{u}(L, t) = 0 \tag{6}$$

where $\bar{x} = x/L$, $\bar{t} = t/2L(\rho/T_o)^{1/2}$, $\bar{f} = \bar{f}(\bar{x}, \bar{t})L/T_o$, $\beta = \eta L/(\rho T_o)^{1/2}$, E = elastic modulus of string, ρ = mass/unit length.

Assuming an approximate solution consisting of first M terms of the modes of the (corresponding) linear string,

$$\bar{u}(\bar{x}, \bar{t}) = \sum_{n=1}^{M} b_n(\bar{t}) \sin n\pi\bar{x} \tag{7}$$

Substituting Eq. (7) into Eq. (5), multiplying by $\sin m\pi\bar{x}$, and integrating from 0 to 1, one obtains a set of M simultaneous nonlinear but ordinary differential equations for $b_n(t)$;

$$(d^2 b_n/d\bar{t}^2) + 2\beta(db_n/d\bar{t}) = -\left[1 + \alpha \sum_{k=1}^{M} k^2 b_k^2\right] \cdot (2n\pi)^2 b_n + 8\gamma \int_0^1 \bar{f}(\bar{x}, \bar{t}) \sin n\pi\bar{x}\, d\bar{x}, \qquad n = 1, 2, \ldots M$$

where

$$\gamma = L/U; \quad \alpha = (AE\pi^2/4T_o)(1/\gamma^2) \tag{8}$$

These equations can be solved numerically without difficulty if the associated generalized forces

$$F_n(t) = \int_0^1 \bar{f}(\bar{x}, \bar{t}) \sin n\pi\bar{x}\, d\bar{x} \tag{8a}$$

are given numerically.

This can be accomplished easily since $\bar{f}(\bar{t}, \bar{x})$ can be readily simulated in a manner described in Sec. II. Note that the integral in $F_n(t)$ can be carried out analytically because $\bar{f}(\bar{t}, \bar{x})$ is a sum of cosine functions; this results in a significant saving in computer time in simulating the generalized forces.

The result of the analysis will be shown in a diagram where the root mean square (rms) of the response is plotted against that of the excitation. Since, however, the statistical fluctuation in the rms of the simulated excitation process will undoubtedly reflect on the rms of the simulated response process, both are estimated by means of temporal average although the theoretical value of the rms for the excitation process is known [and equal to σ as in Eq. (4)]. For this purpose, Eq. (7) is used for the response upon computing $b_n(t)$ and Eq. (2) for the excitation.

As an example, a nondimensionalized pressure field, $\bar{f}(\bar{x}, \bar{t})$ with a nondimensionalized generalized spectral density

$$\bar{\Phi}_o(\bar{\omega}, \bar{k}) = ac|\bar{\omega}|/[\pi^2(a^2 + \bar{\omega}^2)(c^2\bar{\omega}^2 + \bar{k}^2)] \tag{9}$$

is applied to the string. Equation (9) is equivalent to the well-known cross-spectral density $\bar{S}_o(\bar{\omega}, \bar{\xi})$ of the following form often used in the study of dynamic response of a slender structure, e.g. extending along the x-axis under the wind pressure $\bar{f}(\bar{x}, \bar{t})$.

$$S_o(\bar{\omega}, \bar{\xi}) = \bar{S}_o(\bar{\omega}, 0) \exp(-c|\bar{\omega}||\bar{\xi}|) \tag{10}$$

with

$$\bar{S}_o(\bar{\omega}, 0) = a\sigma_f^2/[\pi(a^2 + \bar{\omega}^2)] \tag{11}$$

A result is obtained for a particular set of values of parameters involved ($\beta = 2\pi/10$, $a = 4\pi$, $c = 0.7$ and $\alpha = 0.5$) and shown in Fig. 1 where rms value of the nondimensional displacement $\bar{u} = u/(0.1L)$ at the midspan is plotted against that of the nondimensional excitation $\bar{f} = Lf_o(x, t)/T_o$.

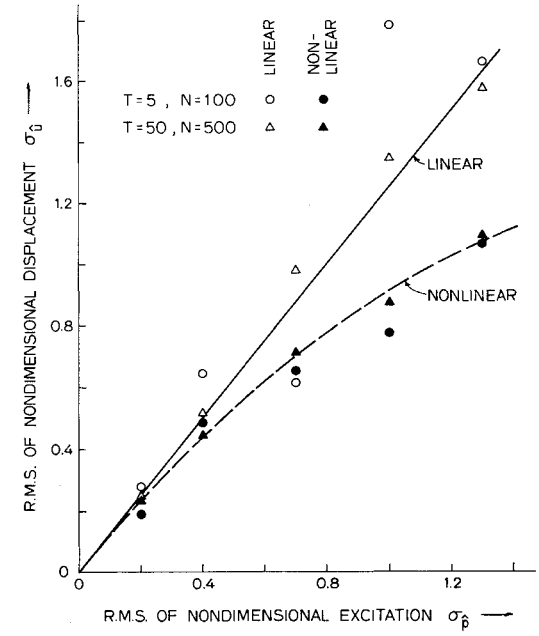

Fig 1 An rms response of nondimensional displacement (string).

The accuracy of the present approach is first checked against the exact solution obtained for the corresponding linear string. Open circles indicate the rms values based on simulated excitation processes consisting of 100 cosine terms ($N = 100$) and on the temporal average computed over $T = 5$ cycles of fundamental period $2L(\rho/T_o)^{1/2}$ of the linear string. Open triangles, however, indicate the values based on $N = 500$ and $T = 50$. It can be shown[2] that theoretically the effect of increasing N on the improvement of accuracy is the same as that of increasing T.

It is evident from the computation for the linear string that a use of $N = 500$ and $T = 50$ produces a reasonable approximation. In fact, the rms value of the nonlinear string (dashed curve) is obtained by interpolating those points (solid triangles) computed with $N = 500$ and $T = 50$. It is interesting to note that the discrepancy between the cases of $N = 500$ and $T = 50$ is much smaller for the nonlinear string, reflecting less violent characteristics of the response behavior of the nonlinear string. Therefore, the values of T and N for a reasonble estimation of linear response are expected to produce an even better estimation of nonlinear response. In the present example, the displacement is dominated by the first mode, both in linear and nonlinear cases, occupying, in the former case, 98% of the total displacement at the midspan.

IV. Response of Nonlinear Plate

For the deflection w of a simply supported rectangular plate (side a and b, respectively, in the x and y directions) with a geometrical nonlinearity, the differential equations and boundary conditions are, in dimensionless form, given by

$$(1/\pi^2)\bar{\nabla}^4\bar{w} = (1/\pi^2)[\bar{\Phi}_{\bar{y}\bar{y}}\bar{w}_{\bar{x}\bar{x}} + \bar{\Phi}_{\bar{x}\bar{x}}\bar{w}_{\bar{y}\bar{y}} - 2\bar{\Phi}_{\bar{x}\bar{y}}\bar{w}_{\bar{x}\bar{y}}] - \lambda\bar{w}_{\bar{t}} - \bar{w}_{\bar{t}\bar{t}} + \bar{p}(\bar{x}, \bar{y}, \bar{t}) \tag{12}$$

$$\nabla^4\Phi = 12(1 - \nu^2)\{w_{xy}^2 - w_{xx}w_{yy}\} \tag{13}$$

$$\left.\begin{aligned} \bar{w}(1, \bar{y}, \bar{t}) = 0 \qquad \bar{w}_{\bar{y}\bar{y}}(1, \bar{y}, \bar{t}) = 0 \\ \bar{w}(\bar{x}, 1, \bar{t}) = 0 \qquad \bar{w}_{\bar{x}\bar{x}}(\bar{x}, 1, \bar{t}) = 0 \end{aligned}\right\} \tag{14}$$

where $t = (t\pi/ab)(D/\rho h)^{1/2}$, $\bar{x} = x/a$, $\bar{\Phi} = \Phi/D$, E = Young's modulus, ρ = mass/unit area, Φ = Airy stress function for membrane stresses, $\lambda = \eta ab/\pi(\rho h D)^{1/2}$, η = coefficient of linear viscous damping.

As in the case of string problem, assume the following approximate solution in terms of the modes of the corresponding linear plate;

$$\bar{w}(\bar{x},\bar{y},\bar{t}) = \sum_{m=1}^{M}\sum_{n=1}^{M} b_{mn}(\bar{t}) \sin m\pi\bar{x} \sin n\pi\bar{y} \tag{15}$$

Equation (15) can be substituted into Eq. (12) together with the stress function $\bar{\Phi}$ evaluated in approximation to obtain M^2 simultaneous nonlinear but ordinary differential equations for $b_{mn}(\bar{t})$, which involve the generalized forces of the form

$$\bar{F}_{mn}(\bar{t}) = (a^2b^2/\pi^2hD)\int_0^1\int_0^1 p(\bar{x},\bar{y},\bar{t}) \sin m\pi\bar{x} \sin n\pi\bar{y}\, d\bar{x}\, d\bar{y} \tag{15a}$$

These generalized forces, however, can easily be simulated since $p(\bar{x},\bar{y},\bar{t})$ can be simulated in terms of the cosine functions [Eq. (2)]. It is important to note again that the "double" integration in Eq. (15a) can be carried out analytically.

If only the first term in Eq. (15) is considered for approximation (computation for linear cases indicates a dominance of the first mode) the solution of $\bar{\Phi}$ satisfying Eq. (13) together with the "average boundary conditions of $\bar{\Phi}$"

$$\int_0^a\int_0^b \frac{\partial u}{\partial x}\,dx\,dy = 0; \qquad \int_0^a\int_0^b \frac{\partial v}{\partial y}\,dx\,dy = 0$$

is given by

$$\bar{\Phi} = b_{11}^2\tfrac{3}{16}\{(1-\nu^2)[(a/b)^2\cos 2\pi\bar{x} + (b/a)^2\cos 2\pi\bar{y}] + 2\pi^2([(b/a)^2+\nu]\bar{y}^2 + [(a/b)^2+\nu]\bar{x}^2)\} \tag{16}$$

where u and v are the in-plane displacement. Substituting Eq. (16) into Eq. (12), multiplying by $\sin\pi\bar{x}\sin\pi\bar{y}$ and integrating over $\bar{x}$ and $\bar{y}$ produces (see Ref. 4 for comparison),

$$\ddot{b}_{11} + \lambda\dot{b}_{11} + c_1 b_{11}[1 + c_2 b_{11}^2] = 4\int_0^1\int_0^1 \bar{p}(\bar{x},\bar{y},\bar{t}) \sin\pi\bar{x}\sin\pi\bar{y}\, d\bar{x}\, d\bar{y} \tag{17a}$$

where

$$c_1 = \pi^2[(b/a)+(a/b)]^2 \tag{17b}$$

$$c_2 = (3/2)\{2\nu + [(3-\nu^2)/2][(b/a)^2+(a/b)^2]\}/(a/b+b/a)^2 \tag{17c}$$

Note that for $a = b$, $c_1 = \omega^2 = (2\pi)^2$ and hence the period T equals to unity. The pressure field considered here is the fluctuating part of the pressure induced by a boundary-layer turbulence. For a numerical example, the semiempirical formula of cross-spectral density associated with a subsonic flow obtained by Bull[5] is used

$$S_{pp}(\xi,\eta,\omega) = S_{pp}(0,0,\omega)\,|R_{pp}(\xi,\eta,\omega)|\exp(i\alpha) \tag{18}$$

where

$$S_{pp}(0,0,\omega) = q_0^2(\delta^*/U_o)[3.7\exp(-2\omega') + 0.8\cdot\exp(-0.47\omega') - 3.4\cdot\exp(-8\omega')]\,10^{-5}$$

for

$$0 \le \omega' < \infty \tag{18a}$$

with ξ = longitudinal separation $|x_1 - x_2|$, η = cross-stream separation $|y_1 - y_2|$, $\alpha = -\omega\xi/U_c(\omega)$ and i = imaginary unit.

The generalized spectral density Φ_o in Eq. (3) can be obtained by performing Fourier transform on Eq. (18) and is given in the following dimensionless form:

$$\bar{\Phi}_o(\bar{\omega},\bar{k}_1,\bar{k}_2) = c\Phi_1(\bar{\omega})\Phi_2(\bar{k}_1,\bar{\omega})\Phi_3(\bar{k}_2,\bar{\omega}) \tag{19}$$

where c is a constant and

$$\bar{\Phi}_1(\bar{\omega}) = \begin{cases} 1.0 - 0.296\exp(-2\bar{\omega}\bar{\delta}^*/\bar{U}_o) \\ \quad -0.272\exp(0.47\bar{\omega}\bar{\delta}^*/\bar{U}_o) \\ \quad +0.068\exp(-8\bar{\omega}\bar{\delta}^*/\bar{U}_o) \text{ for } \omega \ge 0 \\ 0.296\exp(2\bar{\omega}\bar{\delta}^*/\bar{U}_o) + 0.272\exp(0.47\bar{\omega}\bar{\delta}^*/\bar{U}_o) \\ \quad -0.068\exp(-8\bar{\omega}\bar{\delta}^*/\bar{U}_o) \text{ for } \omega \le 0 \end{cases} \tag{19a}$$

and

$$\Phi_2(\bar{k}_1,\bar{\omega}) = \frac{1}{\pi}\left\{\frac{c_1\bar{\omega}/\bar{U}_o}{(c_1\bar{\omega}/\bar{U}_o)^2 + [10c_1(\bar{\omega}/\bar{U}_o) + k_1]^2}\right\} \tag{19b}$$

$$\Phi_3(\bar{k}_2,\bar{\omega}) = \frac{1}{\pi}\left[\frac{c_2\bar{\omega}/\bar{U}_o}{(c_2\bar{\omega}/\bar{U}_o)^2 + \bar{k}_2^2}\right] \tag{19c}$$

where $c_1 = 0.154$ and $c_2 = 1.54\times 0.715b/a$. Note that these three functions are readily integrable in $\bar{\omega}$, $\bar{k}_1$ and $\bar{k}_2$. The rms of the pressure is $0.0056\,q_o$ where q_o is the dynamic pressure in Eq. (18a).

Experimental measurement made by Bull[6] on a $3.5\times 3.5\times 0.01$ in. steel plate showed that for a turbulent airflow at a velocity of 539 fps the boundary-layer displacement thickness δ^* was 0.172 in. Bull's data is used here except that the plate thickness is taken as 0.004 in. so that nonlinear deflections can be produced. Furthermore, excitations at five different levels, i.e., at a velocity of 181, 256, 330, 400, and 520 fps are considered. An approximate estimate (1/7 power law) indicates δ^*'s to be respectively 0.214, 0.198, 0.188, 0.182, and 0.172 in. In Eq. (17), it is assumed that Poisson ratio $\nu = 0.3$ and damping coefficient $\lambda = 1\%$ of the critical damping for the first mode, a value used by Strawderman[7] and Maestrello.[8] The rms of the generalized force σ_p at five velocity levels are 3, 6, 10, 15, and 25, respectively.

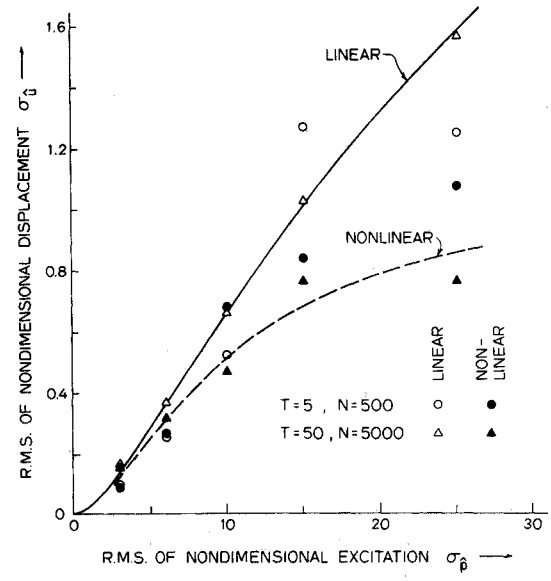

Fig. 2 An rms response of nondimensional displacement (plate).

The rms displacement at the center of the plate is plotted against the rms pressure in Fig. 2 (all in dimensionless form). The relationship between these two quantities is not a straight line even if a linear plate is considered because an increase in the rms pressure is produced by increasing U_o and this in turn will change the shape of the generalized spectral density. The values of N and T to produce a reasonable solution are increased considerably compared with those associated with the string problem. This is because the damping of the system is much lower, or if the structure were considered as a filter, the "band width" is much smaller implying that a larger sample size is needed to maintain the same level of accuracy.

The result in Figs. 1 and 2 indicates that the present method provides a powerful tool in dealing with a type of nonlinear structures considered here. The method in fact can be used for the cases where the intensity of excitation is so high that the perturbation and other standard techniques for nonlinear problems can no longer be applicable.

References

[1] Dowell, E. H., "Transmission of Noise from a Turbulent Layer through a Flexible Plate into a Closed Cavity," *Journal of the Acoustical Society of America*, Vol. 46, No. 1 (Pt. 2), 1969, pp. 238–252.

[2] Shinozuka, M., "Simulation of Multivariate and Multidimensional

Random Processes," *Journal of the Acoustical Society of America*, Vol. 49, No. 1, Jan. 1971, pp. 556–583.

[3] Bolotin, V. V., "Nonconservative Problem of the Theory of Elastic Stability," Pergamon Press, New York, 1963, pp. 280–285.

[4] Chu, H. and Herrman, G., "Influence of Large Amplitude on Free Flexural Vibration of Rectangular Elastic Plates," *Journal of Applied Mechanics*, Vol. 23, No. 4, Dec. 1956, pp. 532–540.

[5] Bull, M. K., "Wall-Pressure Fluctuation Associated with Subsonic Turbulent Boundary Layer Flow," *Journal of Fluid Mechanics*, Vol. 28, Pt. 4, 1967, pp. 719–754.

[6] Bull, M. K., Wilby, J. F., and Blackman, D. R., "Wall Pressure Fluctuation in Boundary Layer Flow and Response of Simple Structure to Random Pressure Fields," A.A.S.U. Rept. 243, Univ. of Southampton, 1963, pp. 1–28.

[7] Strawderman, W. A., "Turbulent-Induced Plate Vibrations, An Evaluation of Finite and Infinite Plate Models," *Journal of the Acoustical Society of America*, 1969, pp. 1294–1307.

[8] Maestrello, L., "Measurement and Analysis of the Response Field of Turbulent Boundary Layer Excited Panels," *Journal of Sound and Vibration*, Vol. 2, 1965, pp. 270–292.

JANUARY 1972 AIAA JOURNAL VOL. 10, NO. 1

Hypersonic Turbulent Skin-Friction and Boundary-Layer Profiles on Nonadiabatic Flat Plates

EDWARD J. HOPKINS,* EARL R. KEENER,† AND THOMAS E. POLEK†
NASA Ames Research Center, Moffett Field, Calif.

AND

HARRY A. DWYER‡
University of California, Davis, Calif.

Direct measurements of skin-friction and velocity profiles were made for $M_e = 5.9$–7.8 at $T_w/T_{aw} = 0.3$ and 0.5. The Van Driest (II), Coles, and finite-difference theories predicted skin friction within about $\pm 10\%$. The theories of Sommer and Short, and Spalding and Chi underpredicted the skin friction by considerably more than 10%. In general, Van Driest's theory also gave the most satisfactory transformations of the velocity profiles onto the incompressible law-of-the-wall and velocity-defect curves.

Nomenclature

A_1, B_1 = constants used in the Van Driest formulas for the skin-friction transformations, see Table 2
A, B = constants used in the Van Driest formulas for the velocity-profile transformations, see Table 3
C_f = local skin-friction coefficient, τ_w/q_e
H = shape factor, δ^*/θ
M = Mach number
N = exponent defined by $U/U_e = (y/\delta)^{1/N}$
p = pressure
q = dynamic pressure
r = temperature recovery factor for turbulent boundary-layer flow, 0.88
Re_θ = Reynolds number based on momentum thickness, $\rho_e U_e \theta/\mu_e$
T = absolute temperature
U = velocity
U_τ = friction velocity, $(\tau_w/\rho)^{1/2}$
y = distance normal to surface from pitot centerline
z = distance normal to surface
δ = boundary-layer thickness determined by extrapolation to $U/U_e = 1.0$ the measured velocity profile in the power-law form, $\log U/U_e$ vs $\log y$
δ^* = displacement thickness $\int_0^{\delta_e} [1-(\rho U/\rho_e U_e)]\, dy$
θ = boundary-layer momentum thickness, $\int_0^{\delta_e} (\rho U/\rho_e U_e [1-(U/U_e)]\, dy$
μ = coefficient of viscosity determined from Keyes' formula[1]
ν = kinematic viscosity
ρ = mass density
σ = Baronti-Libby viscosity function defined in Table 3
τ = local shear stress

Subscripts
aw = adiabatic wall
BL = Baronti-Libby
C = Coles
e = boundary-layer edge
EXP = experimental
f = edge of boundary-layer sublayer, see Table 3
t = total
THE = theoretical
w = wall
∞ = freestream conditions
2 = conditions just downstream of a shock wave

Superscripts
$(\bar{})$ = incompressible or variable transformed to equivalent constant property case
$(\,)'$ = reference condition

Presented as Paper 71–167 at the AIAA 9th Aerospace Sciences Meeting, New York, January 25–27, 1971; submitted February 16, 1971; revision received July 8, 1971.

Index categories: Boundary Layers and Convective Heat Transfer—Turbulent; Supersonic and Hypersonic Flow.

* Research Scientist. Associate Fellow AIAA.

† Research Scientist. Member AIAA.

‡ Associate Professor, Department of Mechanical Engineering. Member AIAA.

Introduction

AN accurate theory for predicting hypersonic turbulent skin friction is required for meaningful design studies of hypersonic vehicles. Unfortunately, all turbulent theories contain some empiricism and are dependent, therefore, upon the accuracy of the experimental data which often show large differences, depending upon the measuring technique. Spalding and Chi found that their semiempirical theory[2] based on skin-friction data from 22 sources (treated without discrimination regarding measuring technique) gave the most accurate skin-friction prediction. In a more recent study by Hopkins et al.,[3] an analysis based on hypersonic data directly measured on cooled flat plates ($T_w/T_{aw} \geq 0.3$) by skin-friction balances indicated that the Coles[4]